

**ACTIVITY AND SUBCELLULAR TRAFFICKING OF THE SODIUM-COUPLED
CHOLINE TRANSPORTER CHT IS REGULATED ACUTELY BY PEROXYNITRITE**

Metta Pinthong, Stefanie A.G. Black, Fabiola M. Ribeiro, Chumpol Pholpramool

Stephen S.G. Ferguson and R. Jane Rylett

Department of Physiology and Pharmacology, Schulich School of Medicine and
Dentistry, University of Western Ontario, London, Ontario, Canada (M.P., S.A.G.B.,
S.S.G.F., R.J.R.); Cell Biology Research Group, Robarts Research Institute, London,
Ontario, Canada (M.P., S.A.G.B., F.M.R., S.S.G.F., R.J.R.); and Department of
Physiology, Faculty of Science, Mahidol University, Bangkok, Thailand (M.P., C.P.)

Running title: High-affinity choline transport regulation by peroxynitrite

Address correspondence to:

Dr. Rebecca Jane Rylett,
Department of Physiology and Pharmacology,
Schulich School of Medicine & Dentistry,
University of Western Ontario,
London, ON, Canada N6A 5C1
Telephone: 519-663-5777 ext 34078
FAX: 519-663-3314
Email: jane.rylett@schulich.uwo.ca

Number of text pages: 25

Number of Tables: 0

Number of Figures: 10

Number of References: 50

Number of Words in Abstract: 190

Number of Words in Introduction: 504

Number of Words in Discussion: 1467

Abbreviations: AD, Alzheimer disease; ACh, acetylcholine; CHT, high-affinity choline transporter protein; ChAT, choline acetyltransferase; DA, diacetate; DCF, 2',7'-dichlorofluorescein; DCFH-DA, 2',7'-dichlorofluorescein diacetate; FeTPPS, 5,10,15,20-tetrakisulfonatophenyl porphyrinato iron (III); KRH, Krebs-Ringer-HEPES; LDH, lactate dehydrogenase; MTT, [3-(4,5-dimethylthiazol-2-yl)-2,5-diphenyltetrazolium bromide]; NO, nitric oxide; OONO⁻, peroxynitrite; RA, all-trans retinoic acid; SIN-1, 3-morpholinonyldimethylamine; O₂⁻, superoxide anion

Abstract

Excess formation of nitric oxide and superoxide by-products (peroxynitrite, reactive oxygen and reactive nitrogen species) attenuates cholinergic transmission potentially having a role in Alzheimer disease pathogenesis. In this study, we investigated mechanisms by which acute exposure to peroxynitrite impairs function of the sodium-dependent, hemicholinium-3 (HC-3)-sensitive choline transporter (CHT) that provides substrate for acetylcholine synthesis. The peroxynitrite generator SIN-1 acutely inhibited choline uptake in cells stably-expressing FLAG-tagged rat CHT in a dose- and time-dependent manner with an $IC_{50} = 0.9 \pm 0.14$ mM and $t_{1/2} = 4$ min. SIN-1 significantly reduced V_{max} of choline uptake without altering the K_m . This correlated with a SIN-1-induced decrease in cell surface CHT protein, observed as lowered levels of HC-binding and biotinylated-CHT at the plasma membrane. Importantly, acute exposure of cells to SIN-1 accelerated the rate of internalization of CHT from the plasma membrane, but did not alter return of CHT back to the cell surface. SIN-1 did not disrupt cell membrane integrity or cause cell death. Thus, the inhibitory effect of SIN-1 on choline uptake activity and HC-3 binding was related to enhanced internalization of CHT proteins from the plasma membrane to subcellular organelles.

Introduction

The principal neurotransmitter used by cholinergic neurons is acetylcholine (ACh), which is synthesized by choline acetyltransferase (ChAT; EC 2.3.1.6) from the precursors choline and acetyl-coenzyme A. The provision of sufficient choline is the rate-limiting step in synthesis of ACh under several conditions, with this choline being delivered into the nerve terminal by the sodium-coupled high-affinity choline transporter (Haga and Noda, 1973; Yamamura and Snyder, 1973) referred to as CHT (Okuda *et al.*, 2000). Dysregulation and/or disruption of CHT function can profoundly affect the levels of ACh synthesized and released, thereby impairing cholinergic neurotransmission (Ferguson *et al.*, 2004). CHT was cloned relatively recently (Okuda *et al.*, 2000; Apparsundaram *et al.*, 2001), and its regulation by phosphorylation (Gates *et al.*, 2004) along with effects of modulation of its subcellular trafficking and compartmentalization on solute transport activity (Ferguson *et al.*, 2003; Ribeiro *et al.*, 2003, 2005, 2006) are active research topics.

Several studies link oxidative and nitrosative modifications of cellular constituents to the pathogenesis of neurodegenerative disorders such as Alzheimer disease (AD), Parkinson's disease and sporadic amyotrophic lateral sclerosis (ALS). Peroxynitrite (ONOO⁻) is a powerful oxidant that can be formed *in vivo* from nitric oxide (NO) and superoxide anion (O₂⁻) (Beckman, 1994). Because it is highly reactive, ONOO⁻ can alter the structure and function of cellular proteins, lipids and other macromolecules by oxidation or nitrosylation. Related to this, increased nitrotyrosine levels have been found in neuronal tissues in AD (Smith *et al.*, 1997) suggesting that ONOO⁻ may be involved in modifying protein function in this disorder.

Authentic ONOO⁻, or ONOO⁻ produced from 3-morpholinosydnonimine (SIN-1), profoundly inhibits activity of some neurotransmitter transporters including the human 5-hydroxytryptamine (5-HT) transporter (SERT) expressed heterologously in COS-7 cells (Bryan-Lluka *et al.*, 2004) and the human dopamine transporter (DAT) expressed in HEK 293 cells (Park *et al.*, 2002). Inducing oxidative stress by treating cells with H₂O₂ also inhibits DAT, but this likely occurs by a different mechanism than inhibition caused by ONOO⁻ (Huang *et al.*, 2003). Oxidative stress mediated by the drug SIN-1 and ONOO⁻, but not by H₂O₂, can affect high-affinity choline uptake activity in synaptosomes isolated from electric organ of *T. marmorata* (Guermonprez *et al.*, 2001). However, the mechanism by which ONOO⁻ impairs choline transport was not investigated.

It was revealed recently that CHT proteins are located predominantly in intracellular compartments, with only a small proportion of total CHT being present at the cell surface (Okuda *et al.*, 2002; Ribeiro *et al.*, 2005; Lips *et al.*, 2002; Nakata *et al.*, 2004). Moreover, altering the relative subcellular localization and trafficking of CHT proteins between the plasma membrane and intracellular compartments appears to be a critical mechanism for regulating its activity (Ribeiro *et al.*, 2005; Apparsundaram *et al.*, 2005). In the present study, we investigated mechanisms by which oxidative stress mediated by the ONOO⁻-generator SIN-1 modulates activity of rat CHT. We demonstrate for the first time that SIN-1 decreases choline uptake activity by changing the dynamics of CHT proteins at the cell surface by modifying their internalization and cycling between the cell surface and subcellular compartments.

Materials and Methods

Materials. 3-morpholinopyrrolidone (SIN-1) was from Biomol Research Labs (Plymouth Meeting, PA), 5,10,15,20-tetrakis(sulfonatophenyl) porphyrinato iron (III) (FeTPPS) was from Calbiochem (San Diego, CA), and [methyl-³H]choline chloride (86 Ci/mmol) and [methyl-³H]hemicholinium-3 diacetate (125 Ci/mmol) were obtained from Perkin-Elmer Life Sciences (Boston, MA). EZ-Link sulfo-NHS-SS-biotin and immobilized NeutrAvidin beads were from Pierce Biotechnology (Rockford, IL). All other chemicals were from Sigma-Aldrich (St. Louis, MO). SH-SY5Y neuroblastoma cells were purchased from American Type Culture Collection (Manassas, VA), HEK 293 Flp-In cells and all cell culture media, fetal bovine serum (FBS) and reagents were from Invitrogen (Burlington, ON, Canada). Rabbit polyclonal and mouse monoclonal anti-nitrotyrosine antibodies were obtained from Upstate Biotechnology (Lake Placid, NY). Protein-A-Sepharose and 2',7'-dichlorofluorescein diacetate (DCFH-DA) were from Sigma-Aldrich (Mississauga, ON, Canada). ECL (Enhanced ChemiLuminescence) immunoblotting reagents were from GE Healthcare Life Sciences (Baie d'Urfé, QC, Canada). The polyclonal antibody against CHT was raised in rabbits by Genemed Synthesis (San Francisco, USA) using a peptide encoding 16 residues (DVDSSPEGSGTEDNLQ) that are conserved at the carboxyl-terminus of human and rat CHT as immunogen; the peptide was conjugated to KLH carrier protein by an amino-terminal cysteine. CHT-specific immunoglobulins were affinity-purified in our laboratory from the crude anti-serum on NHS-Sepharose (Amersham) to which the antigenic peptide had been coupled as the binding element. The specificity of this antibody for detection of CHT was described previously by Ribeiro et al. (2005).

Stable transfection and selection of HEK 293 and SH-SY5Y cells. A FLAG epitope-tag (DYKDDDDK) was added to the amino-terminus of rat CHT by PCR (Ribeiro *et al.*, 2005); the full-length cDNA for CHT ligated to pSPORT was obtained as a gift from Dr. Takashi Okuda (University College London, UK) (Okuda *et al.*, 2000). HEK 293 cell lines stably-expressing FLAG-tagged CHT (referred to as HEK 293-CHT cells) were prepared by introducing FLAG-CHT ligated to pcDNA5 into the Flp Recombinase Target (FRT) site in HEK-Flp-In cells using Lipofectamine 2000 transfection. Cells were grown in Dulbecco's modified Eagle medium (DMEM) with 10% FBS, 0.1% gentamicin and 50 µg/ml hygromycin-B to select stable transformants. SH-SY5Y neuroblastoma cells were transfected with FLAG-tagged rat CHT ligated into pcDNA3.1(-) using Lipofectamine 2000. Stable transformants (referred to as SH-SY5Y-CHT cells) were selected with G418 (500 µg/ml) for 4 weeks, and subsequently maintained in DMEM, 10% FBS, 0.1% gentamicin and G418 (100 µg/ml). Differentiation of SH-SY5Y-CHT cells was induced by supplementing culture media with 10 µM all-trans-retinoic acid (RA) for at least 3 days.

[³H]-choline uptake assay. Cells were washed with Krebs-Ringer-HEPES (KRH) buffer pH 7.4 (in mM: NaCl 124, KCl 5, CaCl₂ 1.5, MgCl₂ 1.2, glucose 10, HEPES 20) and incubated at 37°C in the absence or presence of SIN-1 for times specified in the Results section. Following the treatment period, warm KRH buffer containing [³H]choline (0.5 µM; 0.4 Ci/mmol) was added and incubation continued for 5 min. For kinetic analysis, choline uptake was measured over a range of choline concentrations between 0.5–10 µM with the specific activity of [³H]choline held constant at 0.4 Ci/mmol. [³H]choline uptake was terminated by rapidly washing the cells twice with ice-cold KRH.

Cells were solubilized in 0.1 N NaOH for 30-60 min, then an aliquot was removed for measurement of radioactivity by liquid scintillation spectrometry. Additional aliquots of the solubilized samples were used for quantification of sample protein content using BioRad Protein Assay Dye Reagent. HC-3-sensitive [³H]choline uptake was determined by subtracting choline uptake in the presence of HC-3 from total choline uptake and normalizing to sample protein content to be expressed as pmol / mg protein / 5 min.

Cell toxicity assays. Lactate dehydrogenase (LDH) activity was measured spectrophotometrically in aliquots of cell lysates or culture medium to determine if drug treatments resulted in changes in plasma membrane integrity of cells. LDH activity was monitored as a change in absorbance at 340 nm due to the loss of NADH caused by the reduction of pyruvate to lactate coupled to the oxidation of NADH to NAD⁺ as described previously (Baskey *et al.* 1990). Cells on 12-well plates were treated with SIN-1 at 10, 100 or 1000 μM for 45 min in KRH buffer (pH 7.4) at 37°C. Culture medium was collected for measurement of LDH release from cells, then cells were lysed in 0.5 ml of 1% Triton X-100 to measure total cellular LDH levels. Released LDH activity in culture medium was expressed as a percentage of total cellular LDH activity. Changes in NADH level in assay solutions were monitored at 340 nm at 30 sec intervals for 5 min. The colorimetric 3-(4,5-dimethylthiazol-2-yl)-2,5-diphenyltetrazolium bromide (MTT) assay was used to determine if drug treatments compromised cell viability as described by Calderon *et al.* (1999). Cells in 96-well plates were washed with warm KRH buffer, then incubated in the presence or absence of SIN-1 for 45 min at 37°C. Following incubation of control and treated cells with MTT, cells were rinsed and allowed to air dry before dissolving in 100 μl of 0.04% HCl in isopropanol. The amount of formazan

reaction product formed in each well was determined by measuring absorbance at 570 nm. Negative control wells contained medium alone with no cells. The viability of treated cells was presented as a percentage of control vehicle-treated cells.

[³H]HC-3 binding. Cells were preincubated at 37°C for 45 min in KRH buffer with the addition of vehicle or varying doses of SIN-1, then washed twice with cold KRH and maintained on ice for 10 min. Subsequently, cells were incubated in KRH buffer containing 10 nM [³H]HC-3 (23 Ci/mmol) in the absence (total binding) or presence (non-specific binding) of 1 μM unlabelled HC-3 for 1 h at 4°C. Cells were then washed rapidly twice with ice-cold KRH to remove unbound [³H]HC-3, then digested with 0.1 N NaOH. Aliquots of each sample were taken for radioactivity measurement by liquid scintillation spectrometry and for protein quantification. Specific binding was determined as the difference between total binding and non-specific binding, and normalized to sample protein content to be expressed as fmol / mg protein / hr.

Cell surface protein biotinylation assay. Cells were treated with vehicle or SIN-1 in KRH buffer at 37°C at doses and times indicated in the Results section, and then plasma membrane proteins were biotinylated as described previously (Ribeiro *et al.*, 2005). Briefly, cells were washed 3 times with ice-cold PBS/CM (PBS containing 0.1 mM CaCl₂ and 1 mM MgCl₂), then incubated with sulfo-NHS-SS-biotin (1 mg/ml) in PBS/CM for 1 h at 4°C. Unbound sulfo-NHS-SS-biotin was quenched by washing and incubating cells with 100 mM glycine in ice-cold PBS/CM, followed by washing twice with PBS/CM. Subsequently, biotinylated cells were lysed for 30 min at 4°C in buffer comprised of 1% CHAPS, 0.1 M sodium phosphate buffer, pH 7.2, 10% glycerol and 150 mM NaCl supplemented with DNase (700 U/ml) and protease inhibitors (1 mM

AEBSF, 10 µg/ml each of aprotinin and leupeptin, 25 µg/ml pepstatin A). Aliquots of total cell lysates were incubated at 4°C with NeutrAvidin beads for 2 h with gentle mixing. The beads were then washed with lysis solution, and proteins were eluted from the beads with SDS sample buffer (2% SDS, 10 % glycerol, 0.1 M sodium phosphate buffer, pH 7.2, 0.001% bromophenol blue and 2.5% β-mercaptoethanol) for 5 min at 60°C. Aliquots of biotinylated (avidin-bound) proteins, non-biotinylated proteins and total cell lysates were separated by SDS-PAGE, then proteins were transferred to PVDF membranes. The membranes were blocked with 8% non-fat dry milk in wash buffer (PBS, 0.1% Tween-20) for 30 min, then incubated for 2 h with anti-CHT antibody (1:1000) in wash buffer containing 8% milk. After washing, the membranes were incubated with peroxidase-conjugated anti-rabbit IgG secondary antibody diluted 1:10,000 for 1 h in wash buffer containing 8% milk. Excess antibody was removed by washing and membranes were processed for chemiluminescence detection using the ECL kit. Immunoreactive bands were quantified by densitometry using Scion *Image* software made available by NIH (<http://rsb.info.nih.gov/nih-image/about.html>).

Internalization and recycling of CHT in cells. After the biotinylation of plasma membrane proteins, cells were treated rapidly with either vehicle or 1 mM SIN-1 in warm KRH buffer and transferred to 37°C for varying times to monitor internalization of cell surface proteins. Protein internalization was terminated by transferring culture dishes to 4°C and washing twice with ice-cold PBS/CM. Cells were treated with the membrane-impermeable reducing agent sodium 2-mercaptoethanesulfonic acid (MesNa, 50 mM) in TE buffer (150 mM NaCl, 1 mM EDTA, 0.2% bovine serum albumin, 20 mM Tris-HCl, pH 8.6) to strip biotin from biotinylated proteins that had not undergone

internalization and were retained at the cell surface. For each experiment, the biotin stripping efficiency was assessed on a plate of cells that was treated in parallel, but had been kept on ice to block internalization of cell surface proteins. In the case of experiments designed to assess the movement of previously internalized biotinylated-CHT back to the plasma membrane (“recycling”), biotinylated cell surface proteins were allowed to undergo internalization by incubating cells at 37°C for 15 min, then cells were transferred to 4°C and residual biotin was stripped from proteins that remained at the cell surface. Subsequently, cells were returned to a second round of incubation at 37°C in KRH buffer to allow return of internalized biotinylated proteins to the plasma membrane. Treatments in the presence or absence of SIN-1 were initiated at this latter step for times specified in the Results section. Finally, biotin was removed from previously internalized biotinylated-CHT proteins that had returned (“recycled”) to the cell surface using MesNa in TE buffer as described above thereby allowing measurement of biotinylated proteins retained within the cells. Biotinylated proteins were separated from non-biotinylated proteins on NeutrAvidin beads, then analyzed by SDS-PAGE and immunoblotting as described above.

Detection of tyrosine nitration in CHT. HEK 293-CHT cells were harvested and aliquots containing 1×10^6 cells were transferred to microcentrifuge tubes. Cells were then washed with PBS and resuspended in KRH buffer, following which SIN-1, authentic ONOO⁻ or vehicle were added with immediate mixing. After 30 min incubation at room temperature, cells were washed 3 times with PBS, then centrifuged and lysed in CHAPS-buffer containing protease inhibitors as described above. Immunoprecipitation was used to test for the presence of CHT-containing nitrotyrosine residues in total cell

lysates as described by Tran *et al.* (2003). Briefly, 50 μ l Protein A-Sepharose beads was incubated overnight with either rabbit polyclonal anti-nitrotyrosine antibody (1:125), or mouse anti-FLAG antibody (1:125). Subsequently, aliquots of antibody-bound Protein A-Sepharose were added to cell lysates (400-500 μ g protein) and incubated overnight at 4°C. Antigen-antibody complexes were recovered by centrifugation and bound proteins were eluted in double-strength SDS sample buffer with heating at 60°C for 5 min. Proteins were separated by SDS-PAGE and probed with mouse monoclonal anti-nitrotyrosine antibody (1:1000), or rabbit polyclonal anti-CHT antibody (1:2000), or rabbit polyclonal anti-nitrotyrosine antibody (1 μ g/ml); information from these two forms of immunoblot were compared to evaluate if CHT contained nitrotyrosine residues.

DCF assay. HEK 293-CHT and SH-SY5Y-CHT cells were seeded in 96-well plates at 5×10^4 cells/well and 1×10^5 cells/well, respectively. On the day of experiment, cells were incubated with KRH containing 50 μ M DCFH-DA for 1 h at 37°C, then media was aspirated and cells washed once to remove extracellular DCFH-DA. Cell-permeable DCFH-DA taken up by the cells is converted by intracellular esterases to DCFH by removal of the diacetate (DA) moiety. SIN-1, H₂O₂ or vehicle were added to duplicate wells and fluorescence intensity changes related to oxidation of DCFH to 2',7'-dichlorfluorescein (DCF) were followed at 5 min intervals for 30 min ($\lambda_{\text{Ex}} = 485$ and $\lambda_{\text{Em}} = 510$ nm). This assay was also used to test if SOD, catalase and FeTPPS could reduce DCFH oxidation in cells by adding these agents to culture wells at 5 min prior to the addition of H₂O₂, SIN-1 or vehicle. Changes in fluorescence were calculated by the equation $\Delta F = (F_{t30} - F_{t0})/F_{t0} \times 100$.

Membrane potential measurements. Effects of SIN-1 on membrane potential of SH-SY5Y cells was monitored with the membrane potential-dependent fluorescent dye Oxonal V, as described by Kukkonen et al. (1996). Briefly, cells were harvested in PBS containing 0.02% EDTA, then centrifuged and washed once with Ca²⁺-free KRH buffer. Cell pellets were resuspended in KRH containing 0.5 μM bis-oxonal (DiBAC₄(3)) and incubated for 30 min in the dark at 25°C with gentle mixing to allow loading of dye into cells. Subsequently, aliquots of cell suspension were placed in a stirred cuvette holder heated at 37°C of a PTI fluorescence spectrophotometer, and fluorescence ($\lambda_{\text{Ex}} = 490$ and $\lambda_{\text{Em}} = 530$ nm) was monitored as a function of time. Vehicle or drug (1 mM SIN-1 or 1 mM ouabain) was added at about 5 min when the baseline had stabilized. At the end of each recording, 10 μM gramicidin was added to the cells to induce maximal depolarization for measurement of the maximum fluorescence emission. Changes in fluorescence indicative of changes in membrane potential of the cells were calculated by $\Delta F = (F_{t30} - F_{t0})/F_{t0} \times 100$.

Data analysis. Data are plotted as mean \pm SEM with the number of independent experiments performed shown as *n* values in Fig legends. GraphPad Prism 4 and InStat software were used to perform statistical analyses. For nonlinear regression curve-fitting, one-site competition and one-phase exponential decay were used to determine the IC₅₀ and half-life (*t*_{1/2}) of dose-response and maximal inhibition of choline uptake, respectively. Sigmoid and Michaelis-Menten equations were used to fit dose-response curves and to calculate kinetic parameters (*V*_{max} and *K*_m) of choline uptake, respectively. Statistical significance was determined using either unpaired Student's *t*-test or one-way analysis of variance with Dunnett's posthoc multiple comparison test, as appropriate.

Results

SIN-1 decreases CHT activity

To begin, the effect of SIN-1 on CHT was assessed by measuring HC-3-sensitive, high-affinity choline uptake activity in HEK 293-CHT cells. These experiments revealed that SIN-1 significantly decreases CHT activity in a dose-dependent manner with an IC_{50} of 0.9 ± 0.14 mM, as shown in Fig. 1A. Importantly, the onset of this inhibition is rapid. Cells were incubated in the presence of 1 mM SIN-1 for up to 120 min with maximal inhibition of choline uptake developing with a $t_{1/2}$ of about 4 min. Of note, the inhibitory effect of SIN-1 plateaus at about 50% of control levels and remains constant for up to 120 min (Fig. 1B). Unlike SIN-1, treatment of cells with 1 mM H_2O_2 does not alter CHT activity (Fig. 1A).

To determine if the inhibitory effect of SIN-1 on CHT activity is cell-type specific, we developed lines of SH-SY5Y neuroblastoma cells that stably-express FLAG-tagged rat CHT (SH-SY5Y-CHT cells) for comparison with the HEK 293-CHT cells. As illustrated in Fig. 2A, when compared to wild-type SH-SY5Y cells, two separate SH-SY5Y-CHT cell lines that were tested displayed substantial HC-sensitive choline uptake activity; this activity was about 50% less than that measured in parallel cultures of HEK 293-CHT cells due to lower levels of expression of the transgene in the neural cell lines (data not shown). SH-SY5Y cells grown in the presence of RA differentiate morphologically with the extension of neuritic processes and increased expression of neuron-specific markers (Ecinas *et al.*, 1999; Truckenmiller *et al.*, 2001). Interestingly, HC-sensitive CHT activity was increased significantly by about 5-fold in RA-differentiated SH-SY5Y-CHT cells when compared with undifferentiated SH-SY5Y-CHT

cells ($p < 0.01$) (Fig. 2B). Importantly, HC-insensitive choline uptake was not statistically different between undifferentiated and differentiated cells. As illustrated in Fig. 2B, HC-insensitive choline uptake accounts for about 75% of total choline uptake in undifferentiated cells compared to about 50% of total uptake in differentiated cells. The mechanisms underlying this are not clear, but it does not relate to changes in steady-state levels of CHT mRNA in the cells (data not shown).

Importantly, we determined that SIN-1 also decreases [^3H]choline uptake activity in RA-differentiated SH-SY5Y-CHT cells with the magnitude of effect being similar to that observed in the HEK 293-CHT cells (Fig. 3A). Moreover, neither H_2O_2 (1 mM) nor the NO-donor NOC-5 (1 mM) suppress [^3H]choline uptake in these CHT-expressing cell models (data not shown). Information about the mechanism by which SIN-1 affects CHT activity was obtained by measuring the kinetic parameters of [^3H]choline uptake in vehicle and SIN-1-treated RA-differentiated SH-SY5Y-CHT cells. These experiments reveal that the V_{\max} for choline uptake is reduced significantly from 2.63 ± 0.15 to 2.02 ± 0.13 nmol/mg protein/5 min in vehicle- and SIN-1-treated (1 mM, 30 min) cells, respectively (decrease to 75% of control value; $p < 0.05$, unpaired t -test) (Fig. 3B). The apparent K_m values established for choline uptake in vehicle- and SIN-1-treated cells do not differ significantly (4.46 ± 0.48 and 5.12 ± 0.89 μM , respectively) (Fig. 3B). It is possible, however, that this effect on choline uptake could be due to cellular damage or toxicity induced by SIN-1. Consequently, we used the MTT assay to monitor cell viability and the release of cytoplasmic LDH into cell culture medium to detect changes in plasma membrane integrity. No differences were found between control and SIN-1-treated cells in either the MTT assay or in LDH levels in the culture medium, thereby

establishing that SIN-1 does not compromise cell viability under these experimental conditions (Fig. 3C).

Based on the finding that SIN-1 leads to a rapid and substantial loss of choline uptake activity in CHT-expressing cells, we carried out experiments designed to address three potential mechanisms: (1) changes in the density of transport proteins located at the cell surface, (2) nitration of susceptible tyrosine residues in CHT leading to loss-of-function, or (3) loss of the driving force for choline transport by collapse of the plasma membrane sodium electrochemical gradient or membrane potential.

Effect of SIN-1 on cell surface levels of CHT

For CHT to exert its function of transporting choline into the neuron, it must be inserted into the plasma membrane. Thus, we hypothesized that the SIN-1-induced decrease in choline uptake activity is related to a decrease in the density of CHT proteins at the plasma membrane. To test this, we exposed HEK 293-CHT cells to 1 mM SIN-1 to decrease choline uptake activity by about 50%, then measured the levels of CHT at the cell surface in comparison to vehicle-treated control cells. For this purpose, we used the well-characterized high-affinity choline uptake antagonist HC-3 as a ligand in binding assays as it binds competitively to CHT, but is not a solute for the transporter (Chatterjee *et al.*, 1987). Moreover, these assays were carried out at 4°C to block internalization of CHT proteins from the cell surface to intracellular compartments (Ribeiro *et al.*, 2005). As illustrated in Fig. 4, these experiments revealed that specific binding of a saturating concentration of [³H]HC-3 is decreased in 1 mM SIN-1-treated cells to about 50% of the control levels ($p < 0.01$). Furthermore, at a lower dose (0.1

mM), SIN-1 also significantly decreases [³H]HC-3 binding to about 75% of control levels ($p < 0.01$), which corresponds well with the choline uptake data (data not shown).

To corroborate this finding, we used a second approach to quantify cell surface levels of CHT protein and assess changes following SIN-1 treatment. In these studies, plasma membrane proteins were biotinylated and recovered on NeutrAvidin beads, then CHT was detected and quantified by immunoblotting with anti-CHT antibody (Ribeiro *et al.*, 2005). To begin, we assessed the effect of SIN-1 treatment on the size of the pool of CHT proteins that becomes biotinylated in HEK 293-CHT cells that were incubated at 37°C for varying times with either vehicle or 1 mM SIN-1 during protein biotinylation. In this experimental paradigm, biotinylated-CHT may be located at the cell surface, internalized to subcellular organelles after labeling, or internalized and subsequently returned to the plasma membrane. This combined pool of CHT, termed the “recycling pool”, is a subpopulation of the total cellular CHT proteins and is available for trafficking between cell surface and subcellular organelles to regulate choline uptake activity by fine-tuning plasma membrane CHT levels (Ribeiro *et al.*, 2006). Fig. 5A shows a representative immunoblot, and reveals that SIN-1 substantially reduces the total size of the recycling pool of CHT proteins in a time-dependent manner (Fig. 5A and B). It is also clear from Fig. 5B that the kinetics of biotinylation of CHT proteins in the recycling pool differs in vehicle-treated compared to SIN-1-treated cells; over a 60 min time course, the rate and magnitude of biotinylation of this CHT pool is greater in control cells when compared to cells exposed to SIN-1.

It is important to note from the immunoblot of CHT in Fig. 5A that despite having a calculated molecular mass of about 63-kDa, CHT appears on immunoblots as at least

one, and often two or three, bands with masses of approximately 40-, 50- and 80-kDa. The 50-kDa protein is the predominant species, with the relative abundance of immunoreactive CHT bands varying depending on expression levels of CHT in cells. As shown in Fig. 5A (middle panel, left), in HEK 293-CHT cell lysates, immunoreactive CHT proteins are observed with masses of about 40- and 50-kDa. Of note, biotinylated CHT protein (Fig. 5A middle panel, right) corresponds to the 50-kDa immunoreactive CHT protein. Also included in this experiment for comparison with CHT was assessment of the effects of SIN-1 on another cell surface receptor, the transferrin receptor (TfR), which is known to undergo clathrin-mediated internalization (Hanover *et al.*, 1985). As illustrated in Fig 5A upper panel, SIN-1 also substantially reduces the total size of the biotinylated pool of TfR in a time-dependent manner similar to that observed for CHT.

As shown in Fig. 6A (left panel), SIN-1 significantly decreases the amount of CHT immunoreactivity at the plasma membrane in a dose-dependent manner. This decrease in CHT density at the cell surface develops rapidly with reduced immunoreactivity seen in cells treated with 1 mM SIN-1 for only 5 min when compared to vehicle-treated control cells. There was no change in the total cellular levels of CHT protein between control and SIN-1-treated cells, as illustrated by the immunoblots in Fig. 6A (lower panels). Quantification of this data from multiple independent experiments by densitometry shows that the level of CHT present at the plasma membrane was reduced to about 60% and 75% of control in cells treated for 45 min with 1 and 0.1 mM SIN-1, respectively ($p < 0.01$) (Fig. 6B). SIN-1 treatment had no apparent effect on actin levels on immunoblots of total cell lysates, and actin was not detectable in the biotinylated protein fractions (data not shown). These latter findings

validate the methodology by indicating further that plasma membrane integrity was maintained in SIN-1-treated cells, and that only cell surface proteins are biotinylated.

SIN-1 enhances the internalization of CHT from the cell surface

Although it was predicted initially that CHT proteins would be localized mostly to the plasma membrane from where they transport choline into the cell, it is clear that unlike some other neurotransmitter transporters CHT is distributed primarily in intracellular compartments with only a small proportion at the cell surface. Moreover, CHT present at the cell surface is internalized rapidly into intracellular membranous organelles through the endocytic endosomal pathway (Ribeiro *et al.*, 2006). Thus, it is expected that the steady-state plasma membrane level of CHT protein will be determined by the rates at which it is internalized into subcellular compartments and returned back to the plasma membrane. In the present study, we used the cell surface protein biotinylation approach to assess if SIN-1 alters the rates of either internalization or reinsertion of CHT protein at the plasma membrane. Following biotinylation of cell surface proteins at 4°C in the absence of SIN-1, the profiles for CHT internalization were compared in cells incubated at 37°C in the absence (control) or presence of 1 mM SIN-1 for 5 and 15 min; following this incubation, residual biotin was stripped from proteins that remained at the cell surface to ensure that only internalized biotinylated proteins were detected.

Importantly, the data illustrated in Fig. 7 reveal a statistically-significant increase in the amount of CHT protein internalized from the plasma membrane in SIN-1-treated SH-SY5Y-CHT cells compared to vehicle-treated control cells. At both 5 and 15 min

after the addition of 1 mM SIN-1 to cells at 37°C, the levels of biotinylated CHT were greater than that found in control cells at 37°C (Fig. 7A, lower panel, lane 3 versus lane 5, and lane 4 versus lane 6, $p < 0.001$ and $p < 0.05$, respectively); an immunoblot of the total cell levels of CHT is shown in Fig. 7A (upper panel) to demonstrate equivalent expression of CHT in each group. The amount of internalized biotinylated CHT was normalized to total cell surface levels of biotinylated CHT in cells incubated at 4°C in the absence of SIN-1 (Fig. 7A, lower panel, lane 1). As experimental controls to validate the method: (1) the amount of total cell surface CHT that is biotinylated is shown in Fig. 7A (lower panel, lane 1), and (2) one dish of cells was incubated on ice to show that internalization of the protein was negligible at 4°C (data not shown) and that MesNa efficiently stripped biotin from cell surface proteins (Fig. 7A, lower panel, lane 2). Typically, one CHT immunoreactive band with molecular mass of about 50-kDa was found on immunoblots of SH-SY5Y-CHT cell lysates (Fig. 7A upper panel), in contrast to results obtained with HEK 293-CHT cell lysates (Fig. 5A lower panel). Biotinylated CHT from SH-SY5Y-CHT cells corresponded to the immunoreactive CHT band at about 50-kDa, similar to that seen with HEK 293-CHT cells.

A line graph summarizing data from multiple experiments is given in Fig. 7B showing an approximately 3-fold increase in the amount of internalized CHT in SIN-1-treated cells at 5 min ($30 \pm 0.3\%$) when compared with control ($10 \pm 2.8\%$) ($p < 0.001$). Although still significantly-different ($p < 0.05$), the magnitude of the difference between control and SIN-1-treated cells was less at 15 min incubation under conditions that are permissive for CHT internalization. Of note, the amount of CHT internalized in control cells increased by about 2-fold from 5 to 15 min ($p < 0.05$). By comparison, the amount of

CHT internalized in SIN-1-treated cells did not increase significantly from 5 to 15 min. These data suggest that the initial rate of internalization of CHT is enhanced by exposure of cells to SIN-1, but that this is not sustained as indicated by saturation of internalization at 15 min when compared to control cells.

SIN-1 effect on CHT movement between cell surface and subcellular organelles

Some cell surface solute transporters and receptors traffick repeatedly between the cytoplasm and plasma membrane (Loder and Melikian, 2003; Deken *et al.*, 2003). We demonstrate here, for the first time, that biotinylated CHT that has undergone internalization from the cell surface can be returned constitutively back to the plasma membrane (Fig. 8A). Fig. 8B illustrates that, under the experimental conditions tested, about 40% of internalized biotinylated CHT returned to the cell surface by 15 min. Moreover, when compared to vehicle-treated control cells, the rate of return of internalized CHT back to the cell surface was not altered in SIN-1-treated cells.

Effect of SIN-1 on intracellular oxidative stress

To assess if SIN-1 and its product ONOO⁻ cause an increase in intracellular oxidative stress, the cell-permeable non-fluorescent probe DCFH-DA was used to monitor levels of reactive oxygen species in control, H₂O₂- and SIN-1-treated cells. After diffusing into cells, the DA moiety is cleaved from DCFH by cytoplasmic esterases, and with increasing oxidative stress in cells DCFH can be oxidized to the fluorescent compound DCF. As shown in Fig. 9, both H₂O₂ (500 μM) and SIN-1 (100 μM) significantly increased the fluorescence intensity of DCF, confirming that they are

membrane-permeable oxidizing agents; induction of DCF fluorescence was greater with SIN-1 suggesting that it is a more powerful oxidizing agent than is H_2O_2 . Pretreatment with catalase (100 U/ml), which breaks down H_2O_2 , attenuated increases in DCF fluorescence in cells treated with H_2O_2 , but not in cells treated with SIN-1. These data indicate that the effects of SIN-1 on CHT were not likely mediated by or related to the formation of H_2O_2 . In contrast, treatment of cells with either SOD (100 U/ml) or FeTPPS (25 μ M), which catalyze the decomposition of $ONOO^-$, significantly reduced the SIN-1-induced increase in DCF fluorescence thus supporting the role of $ONOO^-$ in SIN-1 effects on CHT.

Nitration of tyrosine residues in CHT

To determine if susceptible tyrosine residues in CHT undergo nitration in SIN-1-treated SH-SY5Y-CHT cells, we recovered FLAG-tagged CHT proteins from control and treated cell lysates by immunoprecipitation with anti-nitrotyrosine antibodies. Using experimental conditions where SIN-1 reduces CHT activity, we did not find evidence for tyrosine nitration in CHT proteins in cells treated with either SIN-1 or $ONOO^-$ (data not shown). The converse experiment was also performed in which CHT proteins were immunoprecipitated with anti-CHT antibodies and then probed on immunoblot with anti-nitrotyrosine antibodies. No evidence of nitration of CHT in SIN-1-treated cells was observed (data not shown).

Effects of SIN-1 on membrane potential

As the velocity of choline uptake by CHT is coupled to the sodium electrochemical gradient, we tested the hypothesis that the inhibitory effect of SIN-1 on CHT activity is related to changes in membrane potential of the cell caused by inhibition of Na⁺/K⁺-ATPase and collapse of transmembrane ionic gradients. Previous studies demonstrated that Na⁺/K⁺-ATPase activity is decreased substantially by both SIN-1 and ONOO⁻ (Guzman *et al.*, 1995). To test this hypothesis, the effect of SIN-1 on membrane potential of SH-SY5Y cells was evaluated using the bis-oxonal dye. As illustrated in Fig. 10, bis-oxonal fluorescence was not different between vehicle-treated cells and cells treated for 30 min with 1 mM SIN-1. By comparison, treatment of cells with the Na⁺/K⁺-ATPase inhibitor ouabain (1 mM) resulted in increased bis-oxonal fluorescence suggesting that cells are more depolarized.

Discussion

Several novel observations relating to the regulation of CHT function were made in this study: (1) cell surface levels of CHT are reduced by SIN-1 with this correlating to decreased choline uptake activity and HC-3 binding, (2) SIN-1 enhances the rate of internalization of CHT proteins from plasma membrane to subcellular compartments; similar enhancement of internalization of TfR in SIN-1 treated cells was also observed, (3) CHT that has undergone internalization from the plasma membrane to subcellular organelles can return back to the cell surface with the rate of this not altered by SIN-1, (4) SIN-1 effects on CHT function are not related to nitration of tyrosine residues in the protein or to changes in membrane potential that serves as a driving force for solute transport, and (5) RA-mediated differentiation of SH-SY5Y-CHT cells leads to an approximately 5-fold increase in CHT activity and protein content in cells.

Studying biological effects of ONOO^- in cultured cells is technically challenging due to its short half-life (<1 sec at physiological pH) (Radi *et al.*, 2000), thus making the effective exposure time brief and making it difficult to attain the desired dose. Effects of a bolus of ONOO^- may differ from what occurs *in vivo* where ONOO^- is formed slowly and continuously. As an alternative to using ONOO^- directly, SIN-1 (active metabolite of molsidomine) releases equimolar NO^\cdot and $\text{O}_2^\cdot-$ leading to ONOO^- generation in well-oxygenated aqueous solution at physiological pH. This slow continuous production of ONOO^- from SIN-1 resembles processes occurring during inflammation, ischemic injury and excitotoxicity (Darley-Usmar *et al.*, 1992; Li *et al.*, 2002).

It was reported previously that ONOO^- and SIN-1 inhibit high-affinity choline uptake and ACh synthesis in cholinergic synaptosomes (Guermonez *et al.*, 2001), but

the underlying mechanisms were not investigated. The present study shows that acute exposure of HEK 293 and SH-SY5Y cells expressing CHT to 1 mM SIN-1 rapidly inhibits choline uptake to about 50% of control levels; this agrees with a previous report where synaptosomal HC-sensitive choline uptake was decreased to 50% of control by 0.8 mM SIN-1 (Guermonez *et al.*, 2001). We observed that the inhibitory effect of SIN-1 on CHT activity plateaus within minutes and remains stable up to 2 hr. The reason for this is unclear, but as SIN-1 consumes molecular O₂ with NO generation this could potentially deplete O₂ in media thereby limiting the maximal effect of SIN-1. Studies on the dynamics of O₂ consumption relative to NO production from SIN-1 have been published (Freelisch *et al.*, 1989; Ullrich *et al.*, 1997), but the time frame for substantial reduction of O₂ in media occurs over hours rather than a few minutes.

Inhibition of HC-sensitive choline uptake by SIN-1 in both non-neural (HEK 293) and neural (SH-SY5Y) cells indicates that the effect is not cell-type specific. However, comparison of HEK 293-CHT and RA-differentiated SH-SY5Y-CHT cells revealed a difference in sensitivity of cells to inhibitory effects of SIN-1 on CHT activity. Although the redox state of HEK 293 and differentiated SH-SY5Y cells was not addressed in this study, both cellular redox state and GSH levels are important defenses against ONOO⁻ and SIN-1 (Barker *et al.*, 1996; Fass *et al.*, 2004). Of note, RA-treatment can protect PC12 cells from oxidative injury generated by H₂O₂ (Jackson *et al.*, 1991) suggesting that the transition of SH-SY5Y cells to a more differentiated state may contribute to differences in sensitivity of CHT to SIN-1 between HEK 293 and SH-SY5Y cells.

Characteristics of choline uptake measured in SH-SY5Y-CHT cells are similar to those reported in other expression systems such as *Xenopus* oocytes and transiently-

transfected cells. Strikingly, RA-induced differentiation of SH-SY5Y-CHT cells markedly enhances CHT activity and protein levels in parallel with morphological differentiation of the cells. As stable introduction of transgenes into recipient cells using traditional plasmid transfection methods normally results in random integration of the gene into the host genome, the effects of RA-induced differentiation was tested on two separate clonal cell lines. The data show that both cell lines respond similarly to RA suggesting that it is unlikely that the integration site of CHT cDNA is responsible for the RA-induced increase in CHT expression. Further studies are required to elucidate mechanisms by which RA enhances CHT activity and protein levels in SH-SY5Y-CHT cells.

To assess if SIN-1 and its product ONOO⁻ cause intracellular oxidative stress, the cell-permeable probe DCFH-DA was used (Crow, 1997; Martin-Romero *et al.*, 2004). Coupling DCFH measures with oxidant inhibitors and scavengers make it possible to assess oxidant potency and to identify the oxidant mediating SIN-1 effects. Oxidation of non-fluorescent DCFH to its fluorescent product DCF is relatively selective for ONOO⁻ compared to O₂⁻, H₂O₂ or NO thereby allowing ONOO⁻ formation to be monitored. Under the experimental conditions used, it appears that the product of SIN-1 decomposition is ONOO⁻ rather than H₂O₂; catalase (scavenger of H₂O₂) effectively abolished increased DCF oxidation by H₂O₂, but did not alter increased fluorescence of DCF in the presence of SIN-1. The interpretation that SIN-1-induced ONOO⁻ causes oxidative stress is supported by data that SOD (scavenges O₂⁻) and FeTPPS (scavenges peroxynitrite and uncouples the reaction of NO with O₂ to decrease ONOO⁻ formation) inhibited oxidation of DCF by SIN-1. Also, as intracellular DCF is highly oxidized when SIN-1 is added to media, this indicates that intracellular oxidative stress

might contribute to SIN-1 effects. DCF fluorescence induced by SIN-1 is several fold greater than the response to H₂O₂ confirming the potency of pro-oxidant ONOO⁻.

A primary effect of ONOO⁻ on proteins is nitration of tyrosine residues (Beckman *et al.*, 1992). In relation to this, nitrotyrosine immunoreactivity is increased in necropsy AD brain (Smith *et al.*, 1997) indicating that ONOO⁻ may be involved in the disease pathogenesis. Nitrated residues disrupt normal protein function by several mechanisms, such as altering its ability to undergo tyrosine phosphorylation (Berlett *et al.*, 1996; Nomiya *et al.*, 2004), modification of protein conformation (Hodara *et al.*, 2004; Reynolds *et al.*, 2005) and altering susceptibility to proteolysis (Bar-Shai and Reznick, 2006; Hodara *et al.*, 2004). We hypothesized that tyrosine nitration in CHT may induce loss-of-function. Rat CHT contains 31 tyrosines that are potential targets for ONOO⁻-mediated nitration; 12 tyrosines are located in transmembrane domains and 19 are arrayed in extracellular and intracellular loops. Tyrosine nitration in target proteins yields a modification that can be detected immunologically, thus we used anti-nitrotyrosine antibodies to analyze CHT immunoprecipitated from SIN-1-treated cells. We did not find evidence of nitration of tyrosines in CHT. Similar results (i.e. absence of nitrotyrosine-immunoreactive bands after SIN-1 and ONOO⁻ treatment) were found with cholinergic synaptosomes or cell lines that over-express the human dopamine transporter that were exposed to high doses of SIN-1 (Guermonprez *et al.*, 2001; Park *et al.*, 2002). An alternative target in CHT for ONOO⁻ could be oxidation of cysteine thiols.

We show for the first time that SIN-1 decreases choline uptake by increasing CHT internalization without altering its return to plasma membrane, thus lowering cell surface CHT. Cell surface CHT is determined by its internalization rate into endosomal

compartments and the rate of movement of previously internalized or new CHT to plasma membrane. This latter event is critical for increasing cell surface CHT to mediate rapid enhancement of choline uptake after ACh release, thus facilitating transmitter synthesis to maintain neurotransmission (Ferguson and Blakely, 2004; Ribeiro *et al.*, 2006). Dynamic movement of CHT between plasma membrane and cellular organelles in neurons may involve both regulated and constitutive mechanisms with different functional roles (Ribeiro *et al.*, 2006). In this model, constitutive exocytosis-endocytosis maintains a pool of plasma membrane transporters (estimated at 15% of total CHT), while regulated exocytosis of synaptic vesicles delivers CHT to the cell surface during prolonged excitation of cholinergic nerve terminals. An intracellular recycling pool of CHT that can be recruited as needed could explain how cholinergic transmission is maintained during long periods of stimulation (Birks and MacIntosh, 1961). Conversely, changes that enhance CHT internalization and/or decrease its return to plasma membrane could decrease its cell surface levels, lower ACh synthesis and comprise cholinergic communication.

The mechanism by which SIN-1 enhances CHT internalization is unknown, but may involve modification of CHT interaction with cellular proteins and/or endocytic machinery such as adaptor, Rab or clathrin-pathway proteins. After internalization in clathrin-coated pits, CHT appears to be directed to early endosomes as it colocalizes with Rab5 shortly after endocytosis (Ribeiro *et al.* 2005). In addition to its role in endosomal transport, Rab5 may participate in synaptic vesicle recycling/formation and modulate synaptic vesicle-mediated mobilization of CHT thus regulating choline uptake (Ribeiro *et al.* 2003; Ferguson *et al.* 2003). In this study, SIN-1 also increased TfR

internalization from plasma membrane similar to the effect on CHT. TfR is endocytosed by a clathrin-mediated process (Hanover et al., 1985) and although it was shown that SIN-1 decreases cell surface TfR levels (Richardson *et al.*, 1995), a relationship between these events has not been reported. Taken together, our findings suggest that this SIN-1-mediated effect is not specific to CHT, but may be generalized to other cell surface proteins that undergo regulated endocytosis by a clathrin-mediated mechanism.

Acknowledgements

The authors thank Drs. Jeffrey Dixon and Stephen Sims for assistance with, and use of, the PTI fluorescence spectrophotometer for monitoring changes in cell membrane potential.

References

- Apparsundaram S, Ferguson SM and Blakely RD (2001) Molecular cloning and characterization of a murine hemicholinium-3-sensitive choline transporter. *Biochem Soc Trans* 29:711-716.
- Apparsundaram S, Martinez V, Parikh V, Kozak R and Sarter M (2005) Increased capacity and density of choline transporters situated in synaptic membranes of the right medial prefrontal cortex of attentional task-performing rats. *J Neurosci* 25:3851-3856.
- Bar-Shai M and Reznick AZ (2006) Reactive nitrogen species induce nuclear factor-kappaB-mediated protein degradation in skeletal muscle cells. *Free Radic Biol Med* 40:2112-2125.
- Barker JE, Heales SJ, Cassidy A, Bolanos JP, Land JM and Clark JB (1996) Depletion of brain glutathione results in a decrease of glutathione reductase activity; an enzyme susceptible to oxidative damage. *Brain Res* 716:118-122.
- Baskey JC, Colhoun EH and Rylett RJ (1990) Cholinergic but not GABAergic neuronal markers are decreased in primary neuronal cultures treated with choline mustard. *Brain Res* 519:209-216.
- Beckman JS (1994) Peroxynitrite versus hydroxyl radical: the role of nitric oxide in superoxide-dependent cerebral injury. *Ann N Y Acad Sci* 738:69-75.
- Beckman JS, Ischiropoulos H, Zhu L, von der Woerd M, Smith C, Chen J, Harrison J, Martin JC and Tsai (1992) Kinetics of superoxide dismutase- and iron-catalyzed nitration of phenolics by peroxynitrite. *Arch Biochem Biophys* 298:438-445.

Berlett BS, Friguet B, Yim MB, Chock PB and Stadtman ER (1996) Peroxynitrite-mediated nitration of tyrosine residues in Escherichia coli glutamine synthetase mimics adenylation: relevance to signal transduction. *Proc Natl Acad Sci U S A* 93:1776-1780.

Birks RI and MacIntosh FC (1961) Acetylcholine metabolism of a sympathetic ganglion. *Can J Biochem Physiol* 39:787-827.

Bryan-Lluka LJ, Papacostas MH, Paczkowski FA and Wanstell JC (2004) Nitric oxide donors inhibit 5-hydroxytryptamine (5-HT) uptake by the human 5-HT transporter (SERT). *Br J Pharmacol* 143:63-70.

Calderon FH, Bonnefont A, Munoz FJ, Fernandez V, Videla LA and Inestrosa NC (1999) PC12 and neuro 2a cells have different susceptibilities to acetylcholinesterase-amyloid complexes, amyloid25-35 fragment, glutamate, and hydrogen peroxide. *J Neurosci Res* 56:620-631.

Chatterjee TK, Cannon JG and Bhatnagar RK (1987) Characteristics of [3H]hemicholinium-3 binding to rat striatal membranes: evidence for negative cooperative site-site interactions. *J Neurochem* 49:1191-1201.

Crow JP (1997) Dichlorodihydrofluorescein and dihydrorhodamine 123 are sensitive indicators of peroxynitrite in vitro: implications for intracellular measurement of reactive nitrogen and oxygen species. *Nitric Oxide* 1:145-157.

Darley-Usmer VM, Hogg N, O'Leary VJ, Wilson MT and Moncada S (1992) The simultaneous generation of superoxide and nitric oxide can initiate lipid peroxidation in human low density lipoprotein. *Free Radic Res Commun* 17:9-20.

- Deken SL, Wang D and Quick MW (2003) Plasma membrane GABA transporters reside on distinct vesicles and undergo rapid regulated recycling. *J Neurosci* 23:1563-1568.
- Encinas M, Iglesias M, Llechna N and Comella JX (1999) Extracellular-regulated kinases and phosphatidylinositol 3-kinase are involved in brain-derived neurotrophic factor-mediated survival and neuritogenesis of the neuroblastoma cell line SH-SY5Y. *J Neurochem* 73:1409-1421.
- Fass U, Panickar K, Williams K, Nevels K, Personett D and McKinney M (2004) The role of glutathione in nitric oxide donor toxicity to SN56 cholinergic neuron-like cells. *Brain Res* 1005:90-100.
- Freelisch M, Ostrowski J and Noack E (1989) On the mechanism of NO release from sydnonimines. *J Cardiovasc Pharmacol* 14 Suppl 11:S13-22.
- Ferguson SM, Savchenko V, Apparsundaram S, Zwick M, Wright J, Heilman CJ, Yi H, Levey AI and Blakely RD (2003) Vesicular localization and activity-dependent trafficking of presynaptic choline transporters. *J Neurosci* 23: 9697-9709.
- Ferguson SM, Bazalakova M, Savchenko V, Tapia JC, Wright J and Blakely RD (2004) Lethal impairment of cholinergic neurotransmission in hemicholinium-3-sensitive choline transporter knockout mice. *Proc Natl Acad Sci USA* 101: 8762-8767.
- Ferguson SM and Blakely RD (2004) The choline transporter resurfaces: new roles for synaptic vesicles? *Mol Interv* 4:22-37.
- Gates J Jr, Ferguson SM, Blakely RD and Apparsundaram S (2004) Regulation of choline transporter surface expression and phosphorylation by protein kinase C and protein phosphatase 1/2A. *J Pharmacol Exp Ther* 310:536-545.

Guermouprez L, Ducrocq C and Gaudry-Talarmin TM (2001) Inhibition of acetylcholine synthesis and tyrosine nitration induced by peroxynitrite are differentially prevented by antioxidants. *Mol Pharmacol* 60:838-846.

Guzman NJ, Fang MZ, Tang SS, Ingelfinger JR and Garg LC (1995) Autocrine inhibition of Na⁺/K⁺-ATPase by nitric oxide in mouse proximal tubule epithelial cells. *J Clin Invest* 95:2083-2088.

Haga T and Noda H (1973) Choline uptake systems of rat brain synaptosomes. *Biochim Biophys Acta* 291:564-575.

Hanover JA, Beguinot L, Willingham MC and Pastan IH (1985) Transit of receptors for epidermal growth factor and transferrin through clathrin-coated pits. Analysis of the kinetics of receptor entry. *J Biol Chem* 260:15938-15945.

Huang CL, Huang NK, Shyue SK and Chern Y (2003) Hydrogen peroxide induces loss of dopamine transporter activity: a calcium-dependent oxidative mechanism. *J Neurochem* 86:1247-1259.

Hodara R, Norris EH, Giasson BI, Mishizen-Eberz AJ, Lynch DR, Lee VM and Ischiropoulos H (2004) Functional consequences of alpha-synuclein tyrosine nitration: diminished binding to lipid vesicles and increased fibril formation. *J Biol Chem* 279:47746-47753.

Jackson GR, Morgan BC, Werrbach-Perez K and Perez-Polo JR (1991) Antioxidant effect of retinoic acid on PC12 rat pheochromocytoma. *Int J Dev Neurosci* 9:161-170.

- Kukkonen JP, Hautala R and Akerman KE (1996) Muscarinic depolarization of SH-SY5Y human neuroblastoma cells as determined using oxonol V. *Neurosci Lett* 212:57-60.
- Li CQ, Trudel LJ and Wogan GN (2002) Genotoxicity, mitochondrial damage, and apoptosis in human lymphoblastoid cells exposed to peroxynitrite generated from SIN-1. *Chem Res Toxicol* 15:527-535.
- Lips KS, Pfeil U, Haberberger RV and Kummer W (2002) Localisation of the high-affinity choline transporter-1 in the rat skeletal motor unit. *Cell Tissue Res* 307:275-280.
- Loder MK and Melikian HE (2003) The dopamine transporter constitutively internalizes and recycles in a protein kinase C-regulated manner in stably transfected PC12 cell lines. *J Biol Chem* 278:22168-22174.
- Martin-Romero FJ, Gutierrez-Martin Y, Henao F and Gutierrez-Merino C (2004) Fluorescence measurements of steady state peroxynitrite production upon SIN-1 decomposition: NADH versus dihydrodichlorofluorescein and dihydrorhodamine 123. *J Fluoresc* 14:17-23.
- Nakata K, Okuda T and Misawa H (2004) Ultrastructural localization of high-affinity choline transporter in the rat neuromuscular junction: enrichment on synaptic vesicles. *Synapse* 53:53-56.
- Nomiyama T, Igarashi Y, Taka H, Mineki R, Uchida T, Ogihara T, Choi JB, Uchino H, Tanaka Y, Maegawa H, Kashiwagi A, Murayama K, Kawamori R and Watada H (2004) Reduction of insulin-stimulated glucose uptake by peroxynitrite is concurrent with tyrosine nitration of insulin receptor substrate-1. *Biochem Biophys Res Commun* 320:639-647.

- Okuda T, Haga T, Kanai Y, Endou H, Ishihara T, Katsura I (2000) Identification and characterization of the high-affinity choline transporter. *Nat Neurosci* 3:120-5.
- Okuda T, Okamura M, Kaitsuka C, Haga T and Gurwitz D (2002) Single nucleotide polymorphism of the human high affinity choline transporter alters transport rate. *J Biol Chem* 277:45315-45322.
- Park SU, Ferrer JV, Javitch JA and Kuhn DM (2002) Peroxynitrite inactivates the human dopamine transporter by modification of cysteine 342: potential mechanism of neurotoxicity in dopamine neurons. *J Neurosci* 22:4399-4405.
- Radi R, Peluffo G, Alvarez MN, Naviliat M and Cayota A (2000) Unraveling peroxynitrite formation in biological systems. *Free Radic Biol Med* 30:463-488.
- Reynolds MR, Berry RW and Binder LI (2005) Site-specific nitration differentially influences tau assembly in vitro. *Biochemistry* 44:13997-14009.
- Ribeiro FM, Alves-Silva J, Volkandt W, Martins-Silva C, Mahmud H, Wilhelm A, Gomez MV, Rylett RJ, Ferguson SS, Prado VF and Prado MA (2003) The hemicholinium-3 sensitive high affinity choline transporter is internalized by clathrin-mediated endocytosis and is present in endosomes and synaptic vesicles. *J Neurochem* 87: 136-146.
- Ribeiro FM, Black SA, Cregan SP, Prado VF, Prado MA, Rylett RJ and Ferguson SS (2005) Constitutive high-affinity choline transporter endocytosis is determined by a carboxyl-terminal tail dileucine motif. *J Neurochem* 94: 86-96.
- Ribeiro FM, Black SAG, Rylett RJ, Prado VF, Ferguson SSG and Prado MAM (2006) The 'ins' and 'outs' of the high-affinity choline transporter CHT1. *J Neurochem* 97:1-12.

Richardson DR, Neumannova V, Nagy E and Ponka P (1995) The effect of redox-related species of nitrogen monoxide on transferrin and iron uptake and cellular proliferation of erythroleukemia (K562) cells. *Blood* 86:3211-3219.

Smith MA, Richey Harris PL, Sayre LM, Beckman JS and Perry G (1997) Widespread peroxynitrite-mediated damage in Alzheimer's disease. *J Neurosci* 17:2653-2657.

Tran MH, Yamada K, Nakajima A, Mizuno M, He J, Kamei H and Nabeshima T (2003) Tyrosine nitration of a synaptic protein synaptophysin contributes to amyloid beta-peptide-induced cholinergic dysfunction. *Mol Psychiatry* 8:407-412.

Truckenmiller ME, Vawter MP, Cheadle C, Coggiano M, Donovan DM, Freed WJ and Becker KG (2001) Gene expression profile in early stage of retinoic acid-induced differentiation of human SH-SY5Y neuroblastoma cells. *Restor Neurol Neurosci* 18:67-80.

Ullrich T, Oberle S, Abate A, and Schroder H (1997) Photoactivation of the nitric oxide donor SIN-1. *FEBS Lett* 406:66-68.

Yamamura HI and Snyder SH (1973) High affinity transport of choline into synaptosomes of rat brain. *J Neurochem* 21:1355-1374.

Footnotes

This research was supported by operating grants to RJR from the Alzheimer Society of Canada (ASC) and Canadian Institutes for Health Research (CIHR). MP was funded by a Scholarship from the Higher Commission on Education, Ministry of Education of Thailand as part of an exchange program between Mahidol University, Bangkok Thailand and the University of Western Ontario, London Canada. SAGB is the recipient of a Doctoral Award from CIHR, and SSGF is a Career Investigator of the Heart and Stroke Foundation of Ontario and holds the CRC in Molecular Neurobiology.

Figure Legends

Figure 1. Acute exposure of HEK 293-CHT cells to SIN-1 inhibits HC-sensitive choline uptake. **(A)** Cells were preincubated with various concentrations of SIN-1 (10 μ M - 2 mM) (■) or with 1 mM H₂O₂ (▲) for 45 min, and **(B)** for various times (5 - 120 min) before choline uptake activity was measured at 0.5 μ M [³H]choline. Data from SIN-1-treated cells are normalized to that obtained for control (vehicle-treated) cells (% of control), and are expressed as the mean \pm SEM of 3-5 independent experiments with triplicate measurements in each experiment. Statistically-significant differences between control and SIN-1-treated cells are denoted as ** for $p < 0.01$.

Figure 2. SH-SY5Y-CHT cells express HC-3-sensitive choline uptake that increases with differentiation. **(A)** Two SH-SY5Y-CHT cell lines were tested revealing CHT activity at about 50% of that found in HEK 293-CHT cells. Wild-type SH-SY5Y cells do not express HC-3-sensitive choline uptake activity constitutively. ***, $p < 0.001$ compared with wild-type cells; ###, $p < 0.001$ compared with HEK 293-CHT cells. **(B)** Differentiation of SH-SY5Y-CHT cells with retinoic acid treatment for 3 days enhances total (black bars), but not HC-insensitive (white bars), choline uptake activity. Net HC-sensitive, CHT-mediated choline uptake was about 5-fold greater in differentiated cells [127.28 ± 17.76 pmol/mg/5 min] compared to undifferentiated cells [26.05 ± 4.68 pmol/mg/5 min]. Data are expressed as mean \pm SEM (n= 4 independent experiments). Total choline uptake in differentiated cells was statistically different from that measured in undifferentiated cells and from HC-insensitive choline uptake in both differentiated and undifferentiated cells, denoted as ** $p < 0.01$. Total choline uptake in undifferentiated

cells and HC-insensitive uptake in differentiated and undifferentiated cells were not significantly different from each other.

Figure 3. SIN-1 inhibits CHT activity in differentiated SH-SY5Y cells. **(A)** [³H]Choline uptake was inhibited in a dose-dependent manner in cells treated for 30 min with SIN-1 at concentrations between 10 μM and 2 mM. Data for SIN-1-treated cells are expressed as percent of vehicle-treated controls, and graphed as mean ± SEM (*n*=4). Statistically-significant differences compared to control are indicated by * *p*<0.05 (one-way ANOVA with posthoc Dunnet's multiple comparison test). **(B)** Kinetic parameters for HC-3-sensitive [³H]choline uptake in control and SIN-1-treated differentiated SH-SY5Y-CHT cells were estimated using [³H]choline concentrations between 0.5 and 10 μM in the absence or presence of 1 μM HC-3. Data are calculated as nmol / mg protein / 5 min and expressed as mean ± SEM from 5 independent experiments with duplicate measurements. Choline uptake data are plotted as a function of [³H]choline concentration, with curves fitted by nonlinear regression analysis using GraphPad Prism 4. SIN-1 (30 min, 1 mM) decreased the maximum velocity (*V*_{max}) of choline uptake by 25% (*, *p*<0.05), with no significant change in affinity (*K*_m). **(C)** The effect of SIN-1 treatment on plasma membrane integrity and cell viability was tested by monitoring LDH release from cells and MTT metabolism, respectively. As can be seen from this panel, treatment of cells for 30 min with SIN-1 up to a concentration of 1 mM did not significantly alter either of these measures compared to vehicle-treated control cells. Data are expressed as mean ± SEM from at least 3 independent experiments.

Figure 4. SIN-1 decreases the binding of [³H]HC-3 to CHT in HEK 293-CHT cells. Cells were treated for 45 min with vehicle or SIN-1 (0.01, 0.1 and 1 mM) prior to measuring total binding of [³H]HC-3 using 10 nM ligand in the absence or presence of 1 μM HC-3 for estimation of non-specific binding. Wild-type HEK 293 cells do not express CHT constitutively as seen by the lack of specific [³H]HC-3 binding. Specific binding was determined as the difference between total binding and non-specific binding, with data normalized to sample protein content. Data are expressed as fmol [³H]HC-3 bound / mg protein and graphed as mean ± SEM from 5 independent experiments with duplicate determinations. Statistically-significant differences compared to control group are indicated by *, $p < 0.05$ or **, $p < 0.01$. Statistically-significant differences compared to 1 mM SIN-1 treatment group are indicated by #, $p < 0.05$.

Figure 5. SIN-1 treatment decreases the size of the total recycling pool of CHT in HEK 293-CHT cells. (A) Cells were incubated for varying times at 37°C in the absence or presence of 1 mM SIN-1 in buffer containing sulfo-NHS-SS-biotin to biotinylate CHT proteins when they are present at the cell surface. A representative immunoblot (middle panel) shows total biotinylated CHT proteins located at the cell surface and internalized into subcellular compartments; total cellular CHT content (non-biotinylated and biotinylated) (left lane, middle panel). A representative immunoblot showing biotinylated TfR is shown for the same experimental paradigm (upper panel) with total TfR in cell lysate illustrated in the left lane, upper panel. Actin immunoreactivity in the biotinylated protein fractions was used as a negative control. The absence of actin in these fractions (lower panel) indicates that CHT or TfR present is recovered as solubilized biotinylated

membrane proteins isolated on NeutrAvidin beads, rather than from contamination of the fractions by intact membranes. Actin immunoreactivity in cell lysates is shown in the left lane, lower panel. (B) A line graph summarizes time course data from densitometric profiles of the biotinylated CHT pool in control and SIN-1-treated cells normalized to total cellular CHT for 5 independent experiments.

Figure 6. SIN-1 treatment decreases the amount of CHT protein at the cell surface. **(A)** HEK 293-CHT cells were incubated at 37°C for 45 min in the absence or presence of SIN-1 (0.01, 0.1 or 1 mM) (**upper panel - left**), or with 1 mM SIN-1 for 5, 15 or 45 min (**upper panel - right**) before biotinylation of cell surface proteins at 4°C for 1 h. Aliquots of lysates (10 µg protein) from parallel sets of cells not undergoing biotinylation were immunoblotted to assess total CHT levels (**lower panel**). **(B)** Immunoblots of biotinylated CHT were quantified by densitometry and relative absorbance units for band densities from SIN-1 treated cells are expressed as a percentage of cell surface CHT obtained for vehicle-treated control cells. Data shown are from 3-5 independent experiments, and represent mean ± SEM. Asterisks (**) indicate that data are statistically different from controls at the level of $p < 0.01$.

Figure 7. SIN-1 increases internalization of CHT from the plasma membrane to subcellular compartments in differentiated SH-SY5Y-CHT cells. **(A)** This representative immunoblot (**lower panel**) shows increased internalization of biotinylated CHT at 5 and 15 min following addition of 1 mM SIN-1 when compared to control cells. **(B)** The line graph displays CHT internalization data normalized to total cell surface CHT computed from 4 independent experiments. Asterisks * and *** indicate data are significantly

different from controls at the level of $p < 0.05$ and 0.001 , respectively, and # ($p < 0.05$) indicates a statistically-significant difference for CHT internalization between 5 and 15 min values in control cells only.

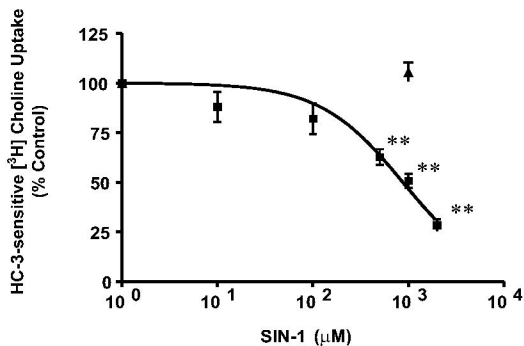
Figure 8. Determination of the return of internalized CHT to the cell surface. After allowing internalization (37°C) for 15 min, two parallel groups of cells were chilled and incubated with MesNa at 4°C to strip biotin from proteins at the cell surface. Cells were then transferred to 37°C and incubated in the presence or absence of 1 mM SIN-1. The decrement in intensity of the internalized-biotinylated CHT band with increasing incubation time (0, 2, 5, and 15 min) at 37°C represents the rate of CHT return back to the plasma membrane. **(A)** Data from a representative experiment are shown. **(B)** The histogram compiles data from 3 independent experiments with data expressed as the percent loss of internalized CHT at each time point, thus allowing assessment of the return of CHT to the cell surface.

Figure 9. DCF assay. HEK 293-CHT cells were incubated with DCFH-DA ($50\ \mu\text{M}$) for 1 hr at 37°C . After washing away excess extracellular DCFH-DA, cells were treated with H_2O_2 (100 and $500\ \mu\text{M}$) or SIN-1 ($100\ \mu\text{M}$) and the changes in fluorescence intensity were monitored at 5 min intervals for 30 min ($\text{Ex} = 485$ and $\text{Em} = 510$). SOD, catalase and FeTPPS were added to some samples at 5 min prior to the treatment. Changes in fluorescence were calculated according to the equation: $\Delta F = (F_{t30} - F_{t0})/F_{t0} * 100$. As expected, SIN-1 is a more powerful oxidizing agent than is H_2O_2 . Catalase ($100\ \text{units/ml}$) significantly reduced the oxidation of DCF in H_2O_2 ($500\ \mu\text{M}$) treated-cells, but

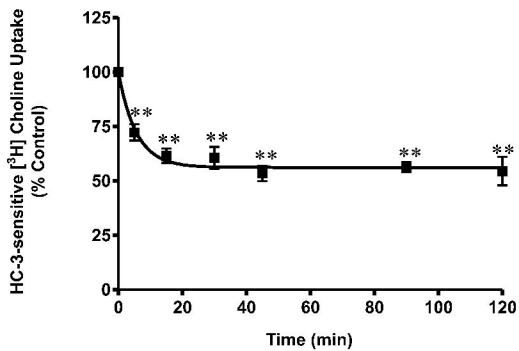
had no effect in cells treated with SIN-1. However, SOD (100 units/ml), which react with O_2^- then inhibits the formation of $ONOO^-$, and FeTPPS (25 μ M), an $ONOO^-$ scavenger, effectively lowered the oxidation of DCF in cells exposed to SIN-1. The bar graphs shown are means \pm SEM (n=4). * $p < 0.05$ and ** $p < 0.01$ compared to control cells.

Figure 10. SIN-1 did not alter cell plasma membrane potential when investigated using bis-oxonal (DiBAC₄(3)). Cell suspensions were incubated in KRH buffer (pH7.4) containing 0.5 μ M bis-oxonal for 30 min at 25°C. Bis-oxonal fluorescence was monitored as a function of time at wavelengths of 490 nm (excitation) and 530 nm (emission) using a PTI fluorescence spectrophotometer. When the baseline had stabilized, vehicle or drug (SIN-1 or ouabain) was added and the fluorescence signal was observed continuously for 30 min. **(A)** The bar graph represents mean \pm SEM of data obtained from 3 independent experiments. **(B)** Representative traces of changes in fluorescence observed during a 30 min incubation with vehicle or drug treatment of cells. Drug or vehicle were added at time = 0 min on these traces, with the baseline having stabilized for several minutes prior to these additions. Gramicidine (10 μ M) was added at the end of each incubation (i.e. at the 30 min time-point) to induce membrane depolarization and observed as a large increase in fluorescence intensity.

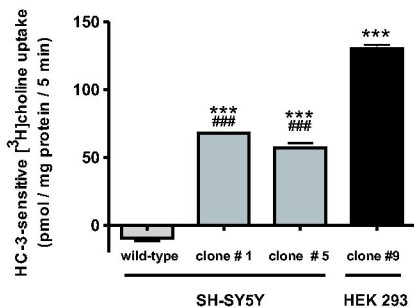
A.



B.



A.



B.

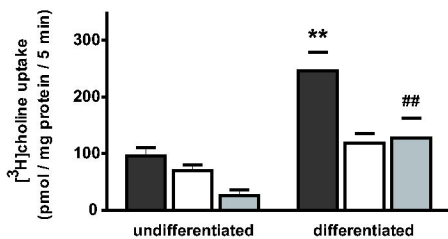
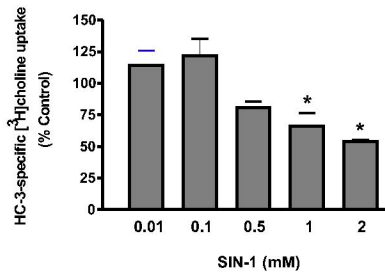
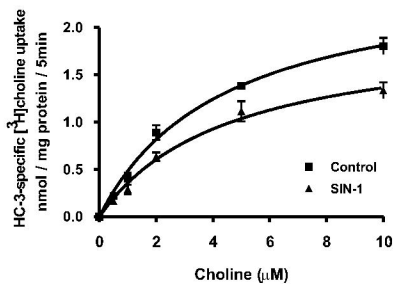


Figure 3

A.



B.



C.

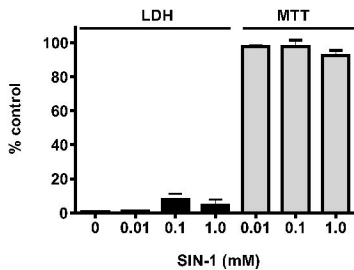
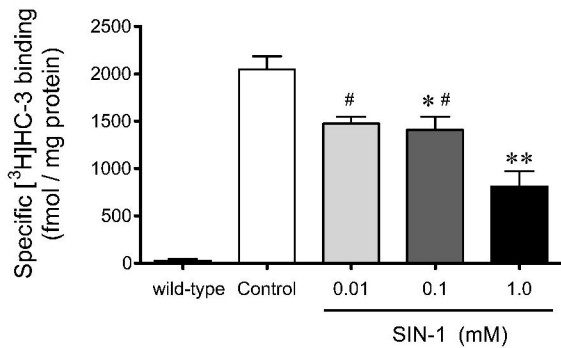
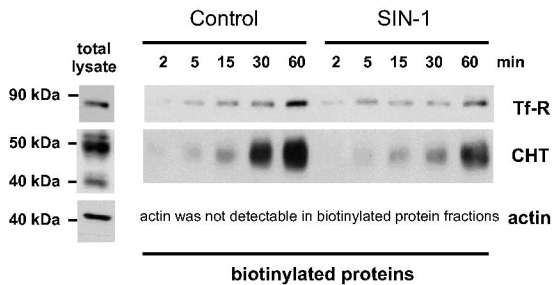


Figure 4



A.



B.

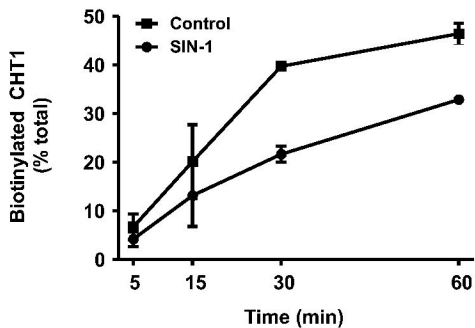
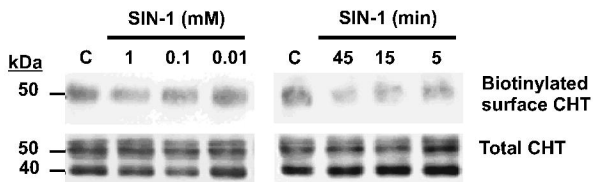
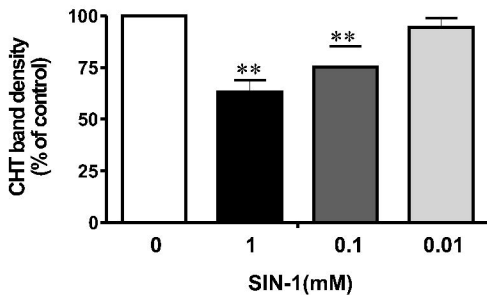


Figure 6

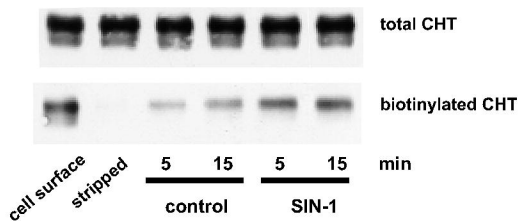
A.



B.



A.



B.

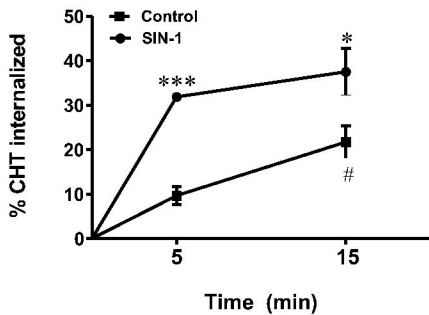
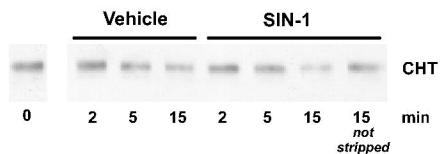


Figure 8

A.



B.

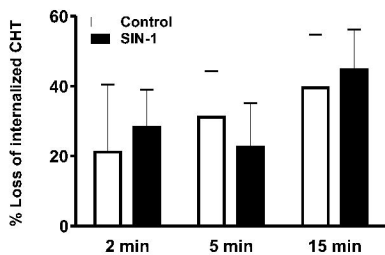


Figure 9

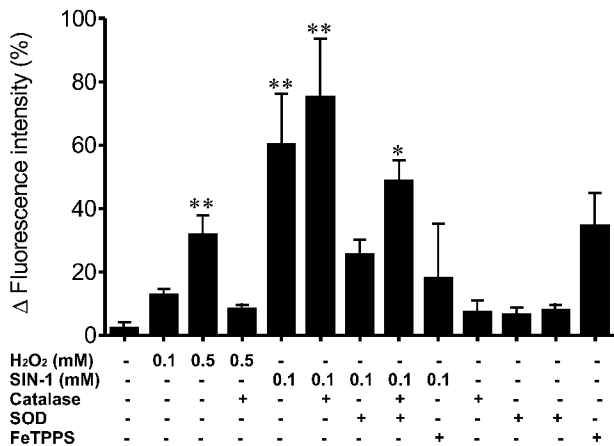
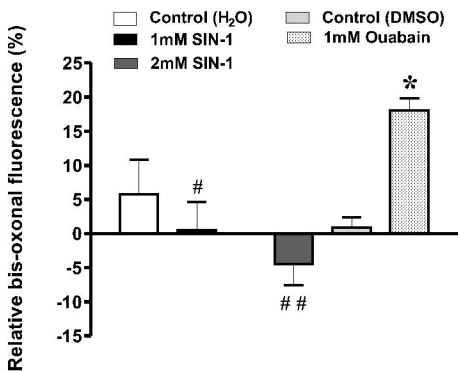


Figure 10

A.



B.

